Converter Lifetime Assessment for Doubly-Fed Induction Generators Considering Derating Control Strategies at Low Rotor Frequencies

Converter Lifetime Assessment for Doubly-Fed Induction Generators Considering Derating Control Strategies at Low Rotor Frequencies

Marcel Morisse[1], Arne Bartschat[2], Jan Wenske[2] and Axel Mertens[1]

[1] Institute for Drive Systems and Power Electronics, Leibniz Universität Hannover, Hannover, Germany
[2] Fraunhofer Institute for Wind Energy and Energy System Technology, IWES, Hannover, Germany

E-mail: marcel.morisse@ial.uni-hannover.de

Abstract. In this paper, various control strategies around the synchronous operating point with the aim to reduce the thermal loading of the rotor-side converter in wind turbines equipped with doubly-fed induction generators are investigated regarding their assets and drawbacks. It is shown that there are various possibilities to prolong the lifetime expectation of the converter regarding its thermal stress by implementing these control strategies. However, every control measure requires a careful design process or a slight adjustment of the system to ensure a positive effect on the overall behaviour of the wind turbine.

1. Introduction

Nowadays, the converter system has one of the largest shares in failures and downtimes of modern wind turbines [1]. It is a well-known fact that in the most common generator type for wind turbines—the doubly-fed induction generator (DFIG)—the synchronous operating point (SOP) can cause a maximum of thermal stress in the rotor-side converter (RSC) [2]. Even though a noteworthy amount of research focuses on the electrical and thermal behaviour of the converter during all operating points, which includes the synchronous operation, there is a lack of work that deals with the possible control strategies to ensure an extended lifetime of the power modules by reducing the thermal stress of the converter during the SOP. To close this gap, this paper deals with the influences that various load-reducing countermeasures have on the lifetime expectation of the RSC. Moreover, unavoidable drawbacks and the application limits of these control strategies are discussed.

Following this introduction, the second section describes the basic properties of the created simulation model of the wind turbine. The applied control strategies are introduced in the third section. In the fourth section, the procedure of the lifetime calculation of the RSC is presented, and the influences of the control measures on the converter's lifetime are shown in section five. Finally, this paper ends with a discussion of the results and an outlook on further possible investigations.

2. Wind turbine model

The model of the wind turbine, which is used for all further investigations, can be seen in fig.1, while the most important parameters of the system are listed in table 1. It consists of a DFIG described in the stator reference dq frame, a back-to-back converter in the rotor circuit, a transformer as well as filter branches at the stator and the converter side to fulfil the requirements of the grid connection.

The mechanical structure is also modelled in detail to achieve an accurate response of the drive train to the generator control. The blade element momentum theory is used to calculate the forces

acting on the rotor blades. The resulting torque at the central hub is then transmitted by a three-stage gear to the torque at the high-speed shaft of the DFIG. Every stage of the combination of one planetary gear and two spur gears is—like the blades—modelled as a spring damper mass system to describe the overall torsional behaviour of the drive train in a suitable way.

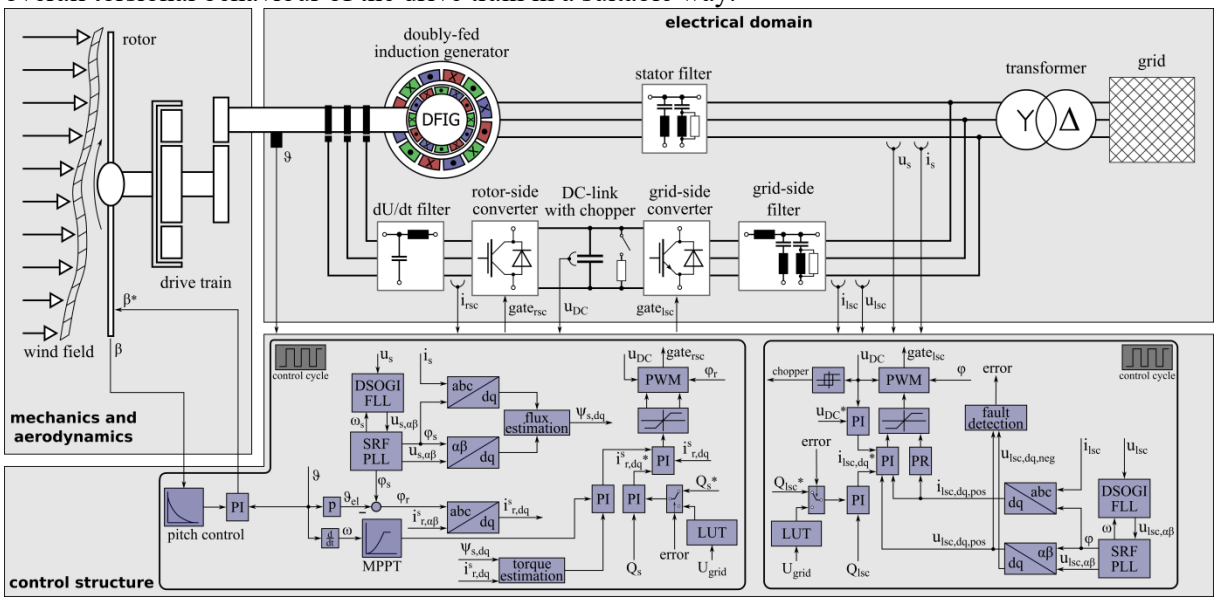

Figure 1. The structure of the wind turbine model.

The control of the IGBT converters is done in the dq frame as well [3]. Hereby, the RSC is oriented towards the stator voltage and controls the electrical torque of the DFIG by an optimal torque curve based on the generator's rotational speed. By controlling the reactive power at the stator terminals, it also partially controls the amount of reactive power at the grid connection. The line-side converter (LSC) is used to control the active power, which is taken from or fed into the grid, depending on the operating point of the generator, by keeping the DC-link voltage at a constant level. It also controls the reactive power at its terminals and thus partially the reactive power at the grid connection.

Table 1. Substantial parameters of the wind turbine system.

System parameters		Electrical parameters	
Rated turbine power	2.19 MW	Transformer primary voltage	3.3 kV
Rated wind speed	10.8 m/s	Transformer secondary voltage	690 V
Optimal tip-speed ratio	6.8	Rated electrical power	2 MW
Maximum power coefficient	0.429	Rated slip range	0.3…-0.2
Turbine speed range	8.75…15 rpm	Generator speed range	1050…1800 rpm
Blade radius	46 m	Generator winding ratio	1 : 2.6
Effective rotor inertia	$8.4 * 10^6$ kg m^2	Rated converter power	400 kW
Gear ratio	120 : 1	DC-link voltage	1.1 kV
Effective turbine inertia	$9.6 * 10^6$ kg m^2	DC-link capacitance	6.6 mF
Overall system efficiency	90 %	Converter switching frequency	2.5 kHz

3. Control strategies

The current-controlled RSC creates a voltage at the rotor terminals with an amplitude and a frequency that is approximately proportional to the slip s, which is a function of the stator angular frequency ω_S and the angular velocity of the generator shaft ω_{mech}:

$$s = \frac{\omega_S - \omega_{mech} \cdot p}{\omega_S} = \frac{\omega_S - \omega_{mech,el}}{\omega_S} = \frac{\omega_R}{\omega_S}. \quad (1)$$

This is necessary to feed the slip-proportional electrical rotor power P_{RSC} into the grid and to achieve the required power factor at the grid connection by providing the magnetizing power of the generator. At the operating point where the slip and the angular frequency of the rotor flux ω_{R} become zero, the RSC has to feed direct currents into the rotor causing a high temperature rise of some of its semiconductors, depending on the amplitude and the direction of the currents. Some selected measures to reduce these temperature peaks, and thereby to prolong the lifetime of the semiconductors, are investigated in the following sections of this abstract.

3.1. Switching frequency reduction

Due to the low fundamental frequencies of the required rotor currents around the SOP, a reduction of the switching frequency of the RSC naturally comes to mind. The resulting decrease of switching power losses then leads to a smaller junction temperature swing of the semiconductors. While this control task is relatively easy to implement, it has to be considered that the current harmonics around the order of the reduced switching frequency have to be damped in accordance with the grid code. Therefore, another notch filter on the stator side tuned to this frequency might be necessary. The reduced switching frequency in this work is half the value of the default switching frequency f_{sw}, which is set to 2.5 kHz.

3.2. Discontinuous modulation method

Another method to reduce the switching losses of the power modules is to use the discontinuous pulse-width modulation (DPWM), as it is described in [4]. This modulation method makes use of the independency of the load voltage on the zero-voltage switching states as long as the star point is not connected. While in a standard—or continuous—pulse-width modulation (PWM) there are four different switching states of a three-phase converter for each reference voltage vector, the DPWM leaves out one of the two possible zero-voltage switching states, depending on the phase angle of the reference voltage and the converter current. This leads to a reduced amount of switching cycles along with a reduced effective switching frequency of approximately two thirds of the one with the continuous PWM.

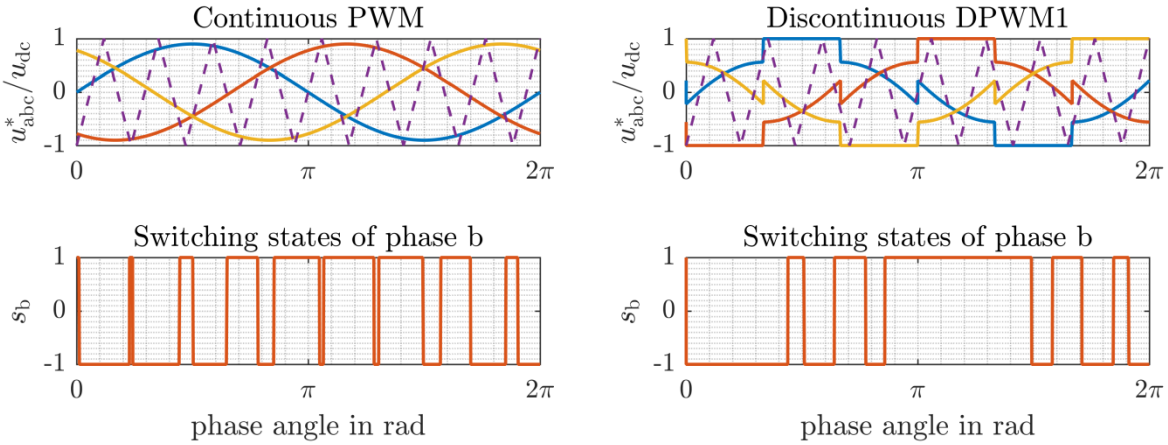

Figure 2. Comparison of a continuous PWM with the DPWM1 method.

The reduction of switching cycles is achieved by alternately maximizing or minimizing the modulation signal of one phase, depending on the phase angle of the voltage and the measured or estimated phase angle of the current. Thereby, the affected phases are each clamped to the positive or negative DC-link connection during 60° of the fundamental period for the DPWM1 and DPWM2 methods which are utilized in this paper. The difference of these two methods is the phase angle of the modulation signal at which the correspondent half-bridge is clamped to the DC link. The DPWM2 method minimizes the switching losses in the phases where the current is at its maximum, which is

assumed to be at 30° lagging behind the voltage phase angle. The DPWM1 method, which is shown in fig.2 for a modulation level of 0.9, ensures that the phase in which the set voltage has its maximum value is prevented from switching.

Unfortunately, the DPWM leads to an increase of the current harmonics at low modulation levels which is a drawback for this application, as the modulation levels are inevitably low around the SOP due to the slip-proportional rotor voltage.

3.3. Rotor current reduction

An additional control lever to reduce both the switching and the conducting power losses is to limit the maximum reference value of the rotor current. A drawback of this method is that the generator is not able to work at its maximum power point during the SOP. Instead, the electrical torque of the DFIG is lower than the optimal torque, and thus the rotor will accelerate faster at rising wind velocities or decelerate slower at falling wind velocities. Around the SOP, the steady-state power generation of the DFIG is then inevitably lower than the optimal power at these wind conditions. Consequentially, a trade-off between power generation and converter protection has to be found.

3.4. Reactive power shifting

The fourth and last control strategy in this paper is based on the power distribution within the wind turbine system with a DFIG. As well as the active power, which is extracted from the wind and partially fed into the grid by the stator and the LSC, the reactive power at the grid connection is also determined by the sum of the reactive power demand of the generator and the converter at the grid. In [5], this is used to enhance the lifetime expectation of the RSC by controlling the LSC to take over some of the reactive power demand of the grid operator. In this paper, the demanded power factor at the grid connection is assumed to be zero, and the LSC is used to compensate part of the reactive power which is needed for the magnetization of the generator. This power is defined by the actual stator voltage $U_\mathrm{S}$and the magnetizing reactance X_μ:

$$Q_\mu = \frac{U_\mathrm{S}^2}{X_\mu}. \tag{2}$$

Equations 3 and 4 show the dependencies of the active and reactive power at the stator terminals on the active and reactive rotor currents $I_\mathrm{R,d}$ and $I_\mathrm{R,q}$, which are the bases of the control design of the RSC.

$$P_\mathrm{S} = \frac{3}{2}\omega_\mathrm{S}\frac{L_\mathrm{h}}{L_\mathrm{S}}(\psi_\mathrm{S,q}I_\mathrm{R,d} - \psi_\mathrm{S,d}I_\mathrm{R,q}). \tag{3}$$

$$Q_\mathrm{S} = \frac{3}{2}U_\mathrm{S,q}(\frac{U_\mathrm{s,q}}{\omega_\mathrm{S}L_\mathrm{S}} - \frac{L_\mathrm{h}}{L_\mathrm{S}}I_\mathrm{R,d}). \tag{4}$$

As these equations are not slip-dependent, the RSC experiences high temperature swings due to the relatively high currents around the SOP. The approach behind the reactive power shifting is that the LSC relieves the RSC by feeding reactive power into the grid in a way that it compensates the magnetizing power demand of the stator. At the SOP, the LSC is providing the entire magnetizing power and the reactive power for the filter branches. Because the LSC is experiencing minimal load conditions around the SOP due to the low slip-dependent active power in the rotor circuit, the increased current of the LSC should not affect its lifetime in a critical way, unless it is strongly undersized compared to the RSC.

4. Lifetime calculation

The aforementioned control strategies will be subsequently examined with regard to their impact on the thermal load and the estimated lifetime of the semiconductors of the RSC. Therefore, a calculation method was utilized which allows a comparison of the effects of the control measures. The process of this method is shown in fig.3.

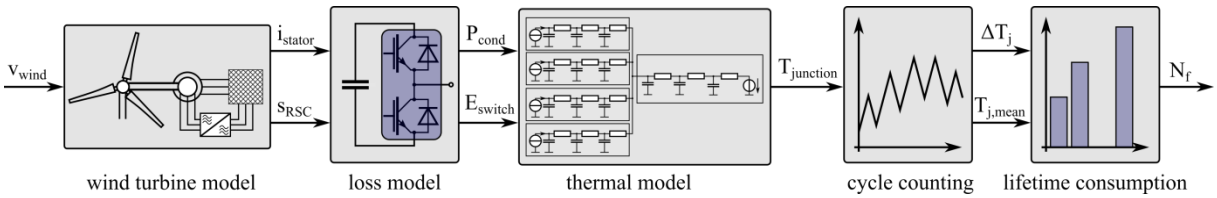

Figure 3. Process diagram for the lifetime calculation of the RSC.

The schematic representation shows the wind turbine model which solves the differential-algebraic equations of the whole system at every time step, depending on the chosen control strategy and the wind velocity vectors as the model's input data. Based on the electrical state variables, the loss model calculates the conducting and switching power losses of every semiconductor during the whole simulation time according to the data sheet values of the power module [6]. These power losses are used to determine the time course of the junction temperature of the semiconductors by using the information about the transient thermal connection of every water-cooled half-bridge to the environment from the same data sheet. The obtained temperature swings are then cumulated and classified according to the heights of the temperature swings and their mean temperatures by a rainflow algorithm [7]. This classification is followed by an estimation of the lifetime consumption based on a power cycling analysis that was experimentally validated in [8] and improved in [9] to fit the failure statistics of modern power modules more accurately.

The usage of the lifetime consumption estimation, however, is subject to some restrictions. The power modules in the referred publications were loaded with DC current and turn-on times of one second and above, while the current of the RSC in the model is pulse-width modulated with a slip-proportional frequency of up to 10 Hz. Even though the formula in [9] allows the consideration of different turn-on times as a consequence of the slip-proportional frequency, this variable is not implemented in the used lifetime calculation at this point. For these reasons, the lifetime calculations in this paper should not be interpreted as absolute values but as an approach to relatively compare the lifetime influences of the different control strategies.

5. Influences of the control strategies on the converter's lifetime

To get comparable results of the impact of the aforementioned control mechanisms, the same time series of the wind speed v_{wind} was used to repetitively simulate the wind turbine model. During these simulations, either the regular control or one of the derating control strategies was activated.

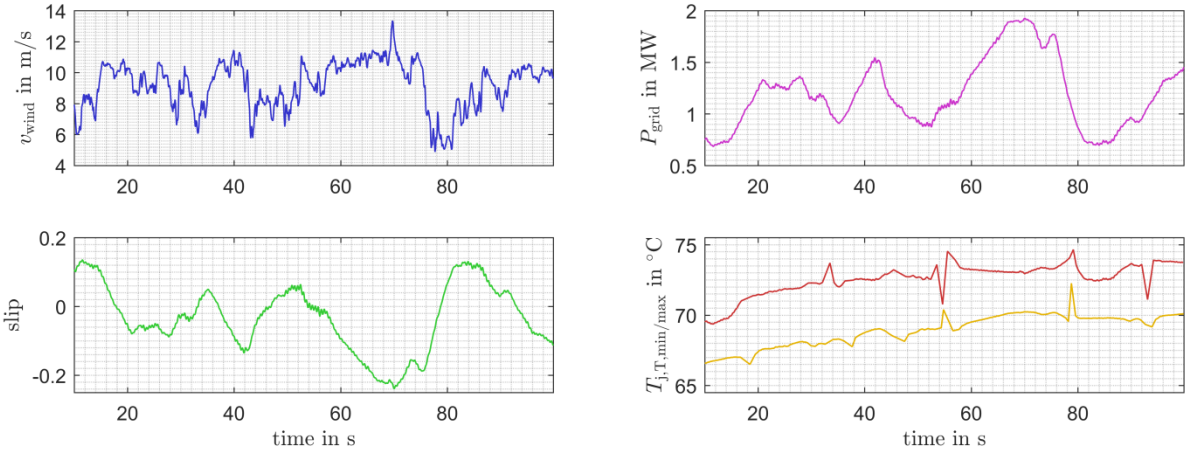

Figure 4. Simulated reference results with the regular control of the RSC.

Some characteristic time courses of the model with the regular control are shown in fig.4 besides the wind speed. In particular, there is the power which is fed into the grid, the slip as a function of the rotor angular velocity, and the maximal and minimal values of the junction temperature of one IGBT

of the RSC—IGBTs are indicated with a subscripted T and diodes with a subscripted D. While for the verification of the control strategies, every semiconductor in every half-bridge of the converter is monitored in the simulation, the thermal behaviour of just one in each case is presented in the following figures for the sake of clarity.

5.1. Switching frequency reduction

The first derating measure for the RSC to be examined is the reduction of the switching frequency. The changing of frequencies is set to happen while the slip is in a predefined range of $|s| \leqq 0.02$ with a small hysteresis of 0.005 to avoid a consecutive activation and deactivation of the control method. As a change in the switching frequency does not notably affect the control performance, the time series of the power and the rotor speed is the same as with the regular control. A visible effect yet occurs at the temperature cycles, which are shown for an IGBT in fig.5, compared with the ones of the regular control. In addition, a lifetime calculation was carried out, and its results are visualised alongside as the consumed lifetime for every classified temperature swing. It can be seen that the greatest temperature swings around the SOP are reduced to a large extent which leads to a consumed lifetime over the simulated time period of 88.4 % of the one with the regular control. The consumed lifetime averaged over all the semiconductors in the RSC compared to the reference is still about 90.4 %.

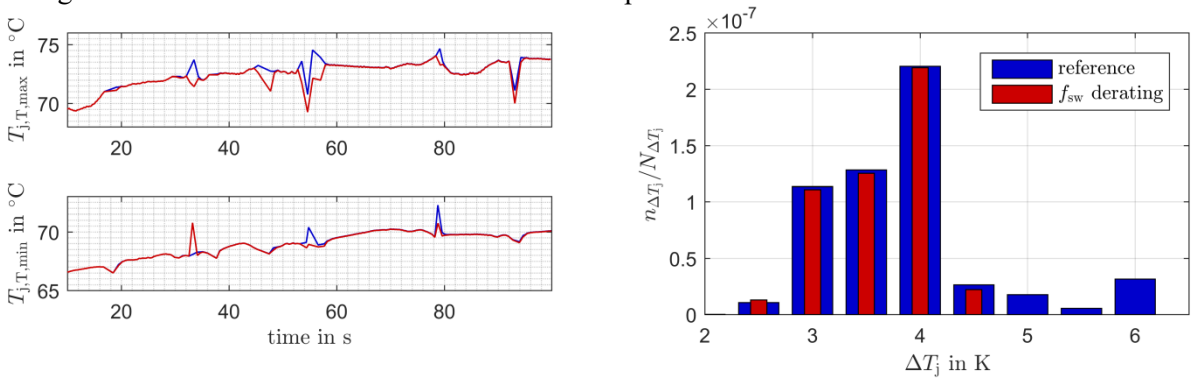

Figure 5. Thermal derating by the switching frequency reduction compared to the reference.

Drawbacks of this method are the already mentioned harmonics spectrum of the stator current that needs to be filtered and a greater current ripple of the converter current which might increase the conducting losses of the RSC. The last-mentioned effect, however, should be more than compensated by halving the switching losses.

5.2. Discontinuous modulation method

As the discontinuous pulse-width modulation methods, the DPWM1 and the DPWM2 were implemented and compared with the continuous PWM regarding the lifetime aspect of the RSC.

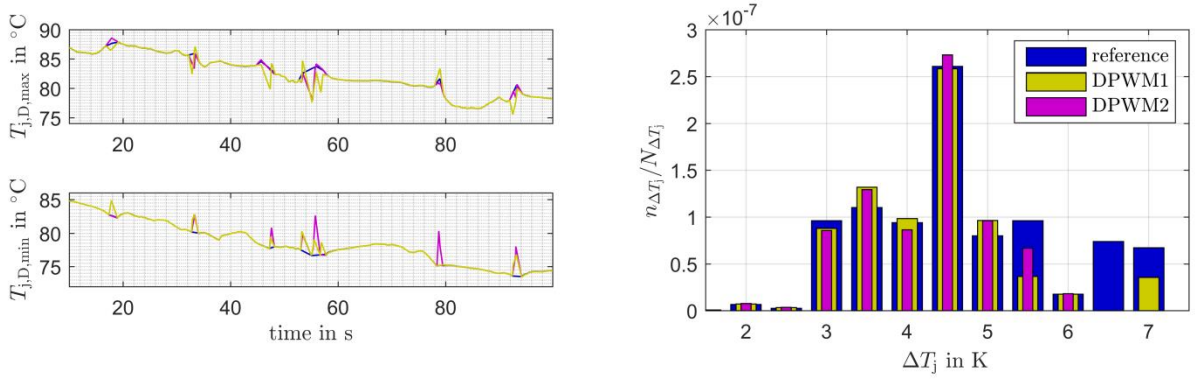

Figure 6. Thermal derating by the DPWM compared to the reference.

The slip range for the change of the modulation methods is the same as for the previously explained switching frequency adaption. Fig.6 shows the resulting temperature cycles as the maximum and minimum values of the junction temperature of one diode. The alternating clamping of one half-bridge of the converter to the DC link reduces the switching losses of the semiconductors of the affected half-bridge. However, the conducting losses of several semiconductors rise due to their prolonged conduction phase. This leads to an increased amount of temperature cycles in the most operating points around the SOP but with a smaller difference of the maximum and minimum temperatures. As a result, the total lifetime consumption of the RSC is reduced. In relative values, the lifetime consumption of the shown diode is approximately 85.3 % of those with the continuous PWM, while the average value of all semiconductors results in a consumption of lifetime compared to the PWM of 90.3 % for the DPWM1 and 93.2 % for the DPWM2.

5.3. Rotor current reduction

The limitation of the maximal rotor current to reduce the thermal heating of the semiconductors of the RSC is the first control strategy that influences the operating points of the generator and its overall control behaviour in a significant way. Due to the electromagnetic torque, which is lower around the SOP than the optimal torque curve, the time courses of the slip and the power in fig.7 differ from the ones with the regular control.

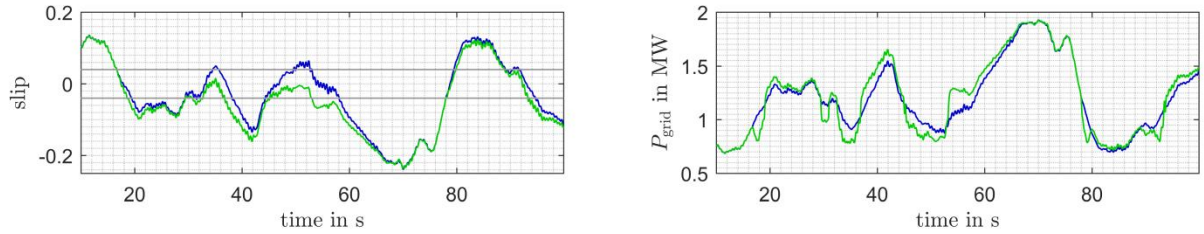

Figure 7. Slip and active power of the current reduction strategy compared to the reference.

The chosen slip range for the control strategy to be operative is within $|s| \leqq 0.04$, again with a small hysteresis of 0.005. The former value is also indicated in fig.7. To avoid the highest temperature peaks, the current control limit is lowered linearly with the slip. It can be seen in fig.7 that the slip deviates strongly from the reference time course at times when the wind speed does not weaken enough to lead to stabilized operating points at sub-synchronous rotor angular velocities. At those times, the power which is fed into the grid is reduced due to the limited electromagnetic torque of the generator. The excess of energy from the wind is then stored in the accelerated masses and dispensed into the grid after the control strategy is deactivated. If the wind speed conditions make the operating point lie around the SOP for a longer time, the wind turbine will operate at a non-optimal tip-speed ratio, thus leading to a decrease of feed-in power. However, in the simulated case of fig.7 the average feed-in power of both time courses differs less than one percent.

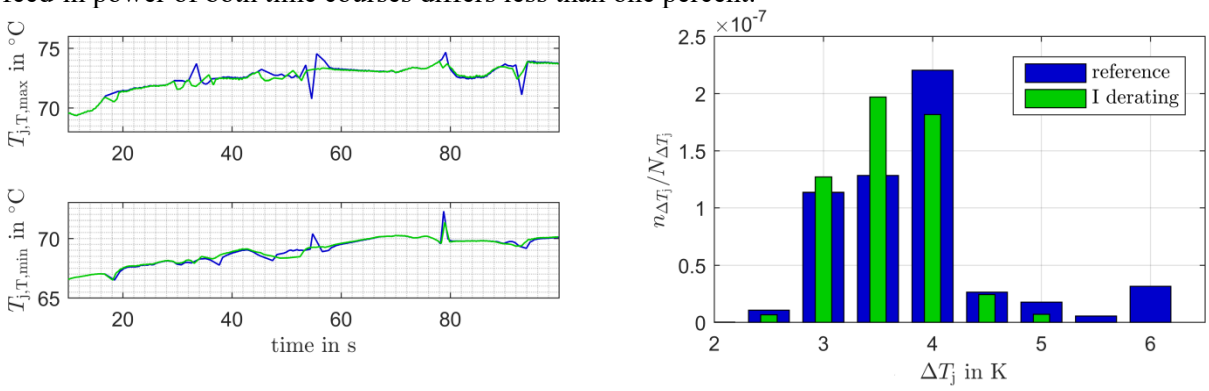

Figure 8. Thermal derating by the current reduction compared to the reference.

Despite the small deviation of the feed-in power, the current reduction control might lead to an increase of the dynamic loads and damaging vibrations of the drive train caused by the relative fast change in the electromagnetic torque. This point should be considered in the design of the control dynamics.

Furthermore, the results of the lifetime comparison of the RSC between the current derating strategy and the reference control are shown in fig.8 again for one IGBT. Most of the very high temperature swings are reduced, as it can be seen on the left side and in the resulting lifetime consumption for the cumulated classified temperature swings on the right side of the figure. Instead, the amount of low temperature swings with a higher fundamental frequency are increased which leads to the higher lifetime consumption of the temperature class of $\Delta T_j = 3.5$ K. This is due to the fact that the operating point with the current reduction control strategy lies more often in a region of greater negative slip values, or higher RSC frequencies respectively, than with the regular control. For a better illustration of these differences, the lifetime consumption of the temperature cycles for both control methods are shown in fig.9 in dependency of the height of the temperature swings and the corresponding mean temperatures.

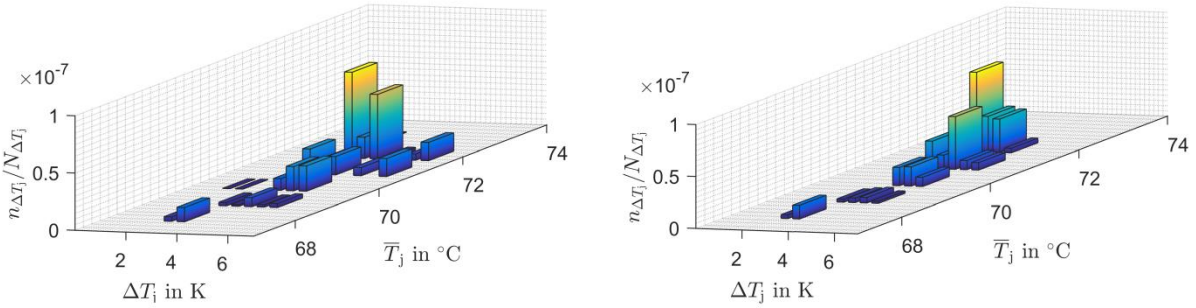

Figure 9. Consumed lifetime of the temperature swings with different heights and mean temperatures of one IGBT with the regular control (left) and the current reduction (right).

Nonetheless, the total consumed lifetime of the observed IGBT of the model with the current derating strategy is 98.1 % of the one with the regular control. The value of the consumed lifetime averaged for all the semiconductors in the RSC is nearly 95.8 % compared to the reference value.

5.4. Reactive power shifting

Two different dependencies of the reactive power shifting from the current slip were implemented and are shown in fig.10. One of them is activated within a slip range of $|s| \leqq 0.08$ and linearly reduces the reactive power the RSC has to deliver by increasing the same amount of reactive power as the set value for the LSC. The second control reduces the reactive power of the RSC to zero from a slip value of $|s| = 0.1$ to$|s| = 0.05$ and keeps it to zero for lower slip values. It has to be ensured that the dynamics of the reactive power controller of the LSC and the RSC have the same time constants to avoid irregular reactive power to be fed into the grid. Alternatively, the possibility of the faster reactive power control of the LSC compared to the RSC might be used to directly measure and control the power factor at the grid connection point of the wind turbine system.

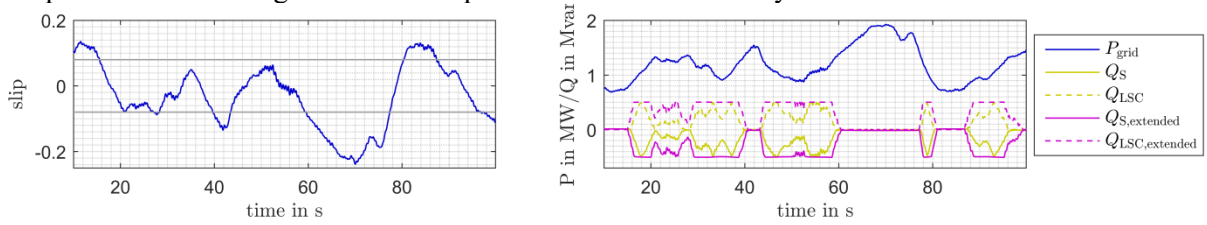

Figure 10. Slip, active power into the grid and reactive power sharing of the RSC and the LSC.

The impact of the control strategies on the thermal behaviour of a diode of the RSC is shown in fig.11.The smoothing of the temperature swings due to the reduction of the current amplitude and the phase angle can be seen on the left side and in the less lifetime consumption of the high temperature swings on the right side of the figure.

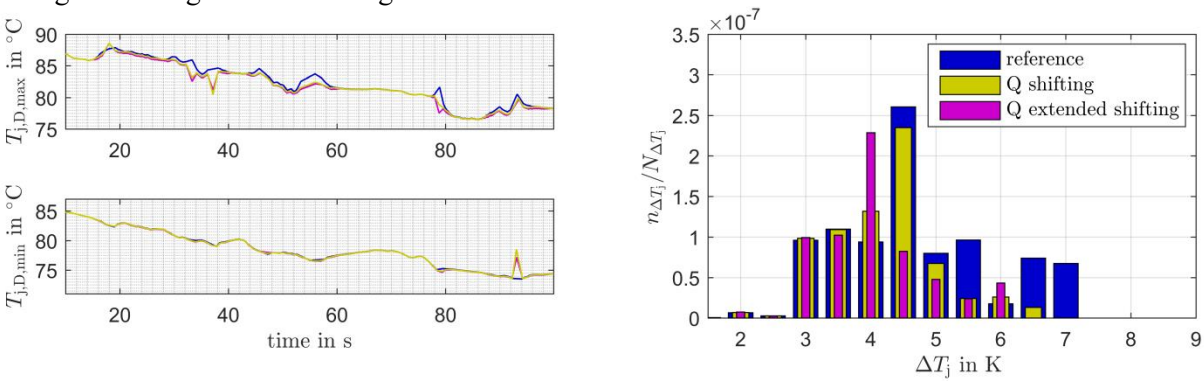

Figure 11. Thermal derating by the reactive power shifting compared to the reference.

According to the lifetime calculations, the expired lifetime of the pictured diode is about 78.8% with the first shifting method and only 70.4 % with the extended reactive power shifting compared to the regular control. Although the lifetime prolongation of the RSC is the greatest for the diodes due to the reduced phase angle of the rotor current and rotor voltage as well as their greater thermal impedance in the power modules, the IGBTs are also less stressed because of the reduced current amplitude. The average lifetime consumption of all semiconductors of the RSC is 86.4 % with the first shifting power control and 79 % with the extended one compared to the reference.

As the LSC is designed only to deliver the active rotor power at the maximal slip value considering the smallest possible power factor demand of the grid operator, which is 0.9 according to the German grid codes, the reactive current values at zero slip might get even higher than the rated current of the LSC, thus leading to a reduced lifetime expectation of the converter on the grid side. While the slip ranges for the control method are the result of a rough estimation in this paper, it is possible to calculate an optimal reactive power share regarding the lifetime of the RSC as well as the one of the LSC by means of the converters' rated current, the reactive power demand of the system's components and the phase-angle dependent loss distribution within the converters. These optimal conditions have to be calculated offline in case of a practical implementation.

6. Conclusion and outlook

The simulations in this paper give a clue about the necessity and the benefits of four different control measures for the RSC in the operating points with low slip values. Every measure is able to reduce the thermal stress the semiconductors of the RSC have to withstand due to currents with high amplitudes and low frequencies. Besides this advantage, there are some drawbacks which have to be considered in the design process of the electrical system. This is for example the extended filter effort on the stator side in case of the frequency reduction and discontinuous modulation methods to fulfil the requirements of the grid operator. Moreover, the reactive power shifting from the RSC to the LSC might lead to a reduced lifetime of the LSC, which makes it necessary to calculate an optimal reactive power sharing of the two converters in advance. At last, the current limitation at low slip values might lead to a non-optimal operating point and as a result to a smaller income of the wind turbine. Therefore, a trade-off between the costs of the RSC and the income due to the feed-in power has to be found. Furthermore, this control strategy might lead to an increase of the dynamic loads at the drive train.

The choice of the most efficient control strategy requires a consideration of the actual wind turbine. However, because of the non-necessity of hardware changes and no major impact on the LSC, the rotor current derating seems to be an efficient solution in prolonging the converter lifetime in any case.

As the simulation time of the whole system under consideration of the switching behaviour of the semiconductors is very slow, only one exemplary time series of wind speed for 100 seconds is used in this paper. The most onshore wind turbines operate in partial load and therefore in the region of the SOP during a large share of their lifetime. A time series of wind velocities, which has steadier wind speeds around the SOP, would probably enhance the effect of the temperature swings of single semiconductors in the RSC and therefore might expose the use of some or all of the presented control strategies in particular.

Furthermore, the possibility to reduce the DC-link voltage around the SOP by a few percent, as the modulation levels of both the RSC and the LSC are relatively low in these operating points, was not examined in this paper. Nonetheless, it is a usable control measure for all the control strategies, except the reactive power shifting. Therefore, its consideration might further reduce the lifetime consumption of the RSC around the SOP.

Additionally, the influence of the control measures on the fault ride-trough capability of the wind turbine is an important aspect which should be addressed in future investigations.

Acknowledgement

The work presented in this paper was carried out within the Fraunhofer-Innovationscluster “Leistungselektronik für regenerative Energieversorgung” (Power Electronics for Renewable Energy Supplies). The project funding by the German Federal State of Lower Saxony by the initiative "Niedersächsisches Vorab" and by the Fraunhofer-Gesellschaft is gratefully acknowledged. The used wind velocity data is based on measured data from the offshore research platform FINO 1 and is supported by the Federal Ministry for Economic Affairs and Energy and Projektträger Jülich.

References

[1] Fischer K and Wenske J 2015 Towards reliable power converters for wind turbines: Field-data based identifications of weak points and cost drivers *EWEA* (Paris, France)
[2] Fuchs F and Mertens A 2011 Steady state lifetime estimation of the power semiconductors in the rotor side converter of a 2 MW DFIG wind turbine via power cycling capability analysis *EPE* (Birmingham, UK)
[3] Abad G, López J, Rodríguez M, Marroyo L and Iwanski G 2011 Doubly Fed Induction Machine: Modelling and Control for Wind Energy Generation *IEEE Press* (New Jersey, USA)
[4] Sujod M Z, Erlich I and Engelhardt S 2013 Improving the Reactive Power Capability of the DFIG-Based Wind Turbine During Operation Around the Synchronous Speed *IEEE Transactions on Energy Conversion Vol. 28 No. 3*
[5] Zhou D, Blaabjerg F, Lau M and Tønnes M 2015 Optimized Reactive Power Flow of DFIG Power Converters for Better Reliability Performance Considering Grid Codes *IEEE Transactions on Industrial Electronics Vol. 26 No. 3*
[6] Semikron Datasheet – Integrated Power Modules – Skiip2403 GB172-4DL V3Rev. 1, 15.05.2014
[7] ASTM E1049-85(2011)e1: Standard Practices for Cycle Counting in Fatigue Analysis 2011 *ASTM International* (Pennsylvania, USA)
[8] Held M, Jacob P, Nicoletti G, Scacco P. and Poech M-H 1997 Fast Power Cycling Test for IGBT Modules in Traction Application *Second International Conference on Power Electronics and Drive Systems* (Singapore)
[9] Bayerer R, Herrmann T, Licht T, Lutz J and Feller M 2008 Model for Power Cycling lifetime of IGBT Modules – various factors influencing lifetime *CIPS* (Nuremberg, Germany)